Analyst

PAPER

View Article Online
View Journal | View Issue

Cite this: *Analyst*, 2018, **143**, 5497

Axially perpendicular offset scheme for obtaining Raman spectra of housed samples in glass bottles with minimized glass-peak background†

Pham K. Duy, Tung D. Vu, Kyeol Chang and Hoeil Chung *

An axially perpendicular offset (APO) scheme based on an axially perpendicular geometrical arrangement of laser illumination and photon detection, enabling spatially offset Raman spectroscopy (SORS), is proposed as a versatile tool for the minimization of the glass background in direct measurements of Raman spectra of samples housed in glass bottles. This strategy is based on the possibility of isolating glass photons from sample photons by properly locating a detector beneath the sample-housing bottle, because glass photons are much more localized near the glass wall while sample photons are widely distributed throughout the bottle. In addition, the curved bottom of the glass vial enabling forming the conical photon-detection volume would be further effective in exclusion of the glass photons in the acquisition of sample spectra. The APO scheme was validated by measuring the Raman spectra of 66% ethanol housed in four glass bottles of different sizes and colors; the measurements were performed by varying the offset distance from 2 mm to 20 mm. The intensity of the glass background decreased rapidly with increasing the offset distance; on the other hand, the variation in the ethanol intensity was relatively insignificant. In all cases, the offset distance of 16 mm minimized the presence of glass background in the spectra, thereby helping to highlight the pure ethanol bands and producing nearly similar sample spectral features regardless of contained bottles. The results of the Monte Carlo simulation were in accordance with the experimental observations, and the suppression of glass photons in the APO scheme was clearly explained and visualized by the simulation.

Received 20th July 2018,
Accepted 11th September 2018

DOI: 10.1039/c8an01344f

rsc.li/analyst

Introduction

Spatially offset Raman spectroscopy (SORS)[1–9] has been demonstrated as an effective and non-destructive analytical tool for direct analysis of samples, especially those contained in various containers. SORS measurements, in which a location of Raman photon detection is spatially away from a point of laser illumination, have been successful in decreasing Raman signals generated by the housing containers, thereby more clearly highlighting spectral features of the contained samples. For example, the group of Matousek performed several SORS experiments for measuring ethylene glycol, neopentyl glycol, and sodium citrate housed in transparent glass bottles, translucent plastics, paper sacks, and colored glass bottles.[10,11]

Taking a step forward, the group of Lendl combined SORS with stand-off Raman measurements, enabling remote detection of samples housed in opaque plastic containers.[12] Meanwhile, an inverse SORS scheme incorporating a reversed excitation collection geometry was also proposed to improve low signal to-noise ratios associated with conventional SORS measurements.[13] One of the most successful SORS applications was the identification of explosives housed in containers for aviation security. Guy T. *et al.* proposed a proper data processing scheme for the reliable identification of samples in a range of different containers. For 97% of the tested samples, the false alarm rate was lower than 0.1%.[14] The minimization of signals associated with containers by SORS was the main factor contributing to accurate identification.

An axially perpendicular offset (APO) scheme, another type of SORS based on an axially perpendicular geometrical arrangement of laser illumination and Raman photon detection, has been demonstrated recently.[15] In this approach, a laser beam is irradiated on a sidewall of a container and Raman photons are detected beneath the bottom of the container. As reported, the APO scheme enabled direct acquisition of reproducible Raman spectra of samples contained in

Department of Chemistry and Research Institute for Convergence of Basic Sciences, College of Natural Sciences, Hanyang University, Seoul, 04763, Korea.
E-mail: hoeil@hanyang.ac.kr; Tel: +82 2 2220 0937; Fax: +82-2-2299-076

†Electronic supplementary information (ESI) available. See DOI: 10.1039/c8an01344f

an oval plastic container, although the container's orientation varied. The intensities of overlapping peaks (attributed to the container) became most consistent at the offset distance of 10 mm, thereby leading to the accurate determination of concentrations of the housed samples, even for different orientations of the oval container.

In this publication, the APO scheme has been further examined as another potential tool for the minimization of background signals emanating from glass bottles, one of the most popular containers, in direct measurements of samples housed in the glass bottles. Because glass has a significant broad peak in the 1800–800 cm^{-1} range, it obviously obscures the spectral features of samples housed in glass bottles, and minimization of the presence of glass background is beneficial for improving the accuracy of the housed sample identification. When a laser beam is irradiated on a side of a sample-containing glass bottle, the generated glass Raman photons are expected to be more localized near the wall while Raman photons of the sample are more widely distributed throughout the bottle. Interestingly, since the bottom of a glass bottle is usually curved, it would be possible to generate a conical-shaped field-of-view (FOV) for Raman photon detection, which would be beneficial to separate the localized glass Raman photons near the bottle wall from the widespread sample photons. Also, a longer offset distance in detection could help further in excluding the glass photons.

This possibility motivated us to investigate how the APO scheme is effective in reducing and minimizing glass background signals. For this purpose, four different glass bottles (three transparent bottles and one brown-colored bottle) of various sizes were chosen as shown in Fig. 1(a), and 66 wt% ethanol samples were transferred into each bottle for APO measurements. APO spectra were collected by regularly increasing offset distances, and subsequent spectral features of glass as well as ethanol were examined. Next, an offset distance providing distinct ethanol peaks with minimal glass background was determined for each case, and the potential dependence of these offset distances on the physical dimensions/characteristics of the housing bottles was investigated.

Another important goal of this study was to provide an acceptable explanation for a reduced glass background in APO measurements. For this purpose, a Monte Carlo simulation was carried out to examine the distributions of both glass and ethanol Raman photons inside the bottles under the APO geometry. Prior to the simulation, the formation of conical FOV was initially tested by illuminating white light through the bottom of a bottle and observing the resulting image, and then focal lengths in each bottle were estimated. Next, the numbers of glass and ethanol photons detected inside the conical detection volume at different offset distances were calculated. Finally, the results of the simulation were compared with the corresponding experimental observations.

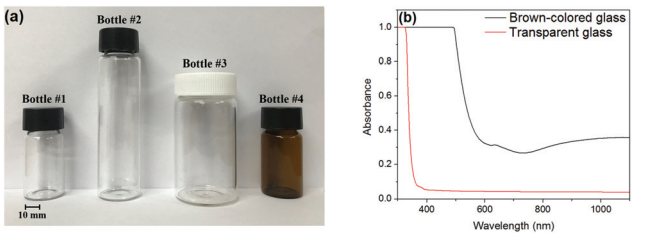

Fig. 1 Four different glass bottles employed in this study (a). Bottle #4 is brown-colored. Visible absorption spectra of the transparent and brown-colored glasses are also shown (b).

Experimental

Preparation of samples and acquisition of spectra

Four different glass bottles, shown in Fig. 1(a), were purchased at a local market. Their sizes and wall thicknesses are summarized in Table 1. Initially to examine light propagation through the curved bottom of the glass bottle, white light generated from a LED flashlight was illuminated through the bottom and then, at the opposite, a location where the clearest real image of the object (the flashlight) was found as described in Fig. S1 (refer to ESI†). Here, the source-to-glass bottom and glass bottom-to-image distances were measured as D_1 and D_2, respectively. Then, the focal length f of the curved bottom for each glass bottle was calculated by using eqn (1) given below. The results are shown in Table S1 (refer to ESI†).

$$\frac{1}{f} = \frac{1}{D_1} + \frac{1}{D_2} \quad (1)$$

As determined, the focal lengths were different from each other, such as 7.4, 7.4, 9.4, and 2.2 cm for bottles #1, #2, #3, and #4, respectively.

A prepared 66 wt% ethanol solution was transferred into each bottle for measurements. Upon the preparation, the ethanol-containing bottles were tightly sealed to prevent possible evaporation of ethanol. For the acquisition of backscattering spectra, a spectrometer (RamanRxn1 unit, Kaiser Optical Systems, USA) equipped with a PhAT probe with a large illumination area (28.3 mm^2, diameter: 6 mm) and a wide photon-detecting area (506.7 mm^2, diameter: 25.4 mm, working distance: 250 mm) was used.[16] For APO measurements, another laser (Invictus, Kaiser) was separately used for excitation, and the spectra were acquired using the same detection probe and spectrometer as those described above. In each case, the detection probe was positioned under the center of the bottle, and the laser illumination point at the left side of the bottle was

Table 1 Physical dimensions of four tested glass bottles employed in this study. Unit: mm

	Diameter	Height	Wall thickness
Bottle #1	27.4	60.4	1.2
Bottle #2	29.9	113.6	1.3
Bottle #3	42.0	82.3	1.5
Bottle #4	27.6	60.4	1.2

varied upward to change the offset distance. The distance between the probe and the bottom of bottle was 180 mm.

The laser wavelength was 785 nm for both backscattering and APO measurements. Raman spectra of each 66% ethanol containing bottle were collected by rotating the bottle to irradiate the laser beam on five different locations on the bottle; this procedure was repeated three times. Therefore, fifteen replicate spectra were acquired for each offset distance. The durations of laser exposure were 2 s and 5 s for the backscattering and APO measurements, respectively. The resolution of the collected spectra was 4 cm^{-1}. As shown in Fig. 1, the diameters of all the employed bottles were larger than that of the detection probe, and bottle #3 had the largest diameter of 42 mm. Bottle #4 was brown-colored while the other bottles were transparent. Baseline correction and normalization of collected spectra were performed using MATLAB version 7.0 (MathWorks Inc., MA, USA).

Monte Carlo simulation

The so called structure factor[17] has been utilized for the Monte Carlo simulation in this study. An attenuation coefficient describing the degree of photon lost at an object needs to be initially determined in this method. When a beam passes through a medium, the intensity of the beam could be attenuated by two causes: absorption and scattering. The scattering and absorption coefficients describe the degrees of photon scattering and absorption, respectively. The sum of the scattering coefficient and the absorption coefficient corresponds to the attenuation coefficient. A more detailed description can be found in the reference indicated above.

Table 2 shows the absorption and scattering coefficients of glass and ethanol used for the simulation. A detailed description of the determination of both coefficients can be found in the ESI.† The number of illuminated photons was 100 000 for the measurements using transparent bottles, while 30% fewer photons were used to illuminate bottle #4, to reflect the attenuation of photons by the brown-colored glass based on the observation of the corresponding visible absorption spectrum, as shown in Fig. 1(b). The diameter of the laser illumination was set at 2.0 mm, corresponding to the actual size of the experimental setup. The conical detection volume was built for each bottle using the determined focal length (equivalent to cone height, Table S1†) and the bottom diameter of 25.4 mm, corresponding to actual size of the detection window in experiments. All the photons reaching the detection cone were simulated and calculated. The simulation was performed using a fully licensed Monte Carlo simulation (Version 2016).[18,19]

Table 2 Parameters of glass and ethanol used in the Monte Carlo simulation

		Absorption coefficient (cm^{-1})	Scattering coefficient (cm^{-1})	Refractive index
Ethanol		6.8×10^{-4}	2.5×10^{-3}	1.362
Glass	Bottle #1	20.8×10^{-4}	1.829	1.518
	Bottle #2		1.689	
	Bottle #3		1.463	
	Bottle #4	67.6×10^{-4}	6.034	

Results and discussion

Examination of the APO spectra of ethanol contained in glass bottles at various offset distances

Fig. 2 shows the APO Raman spectra of 66% ethanol housed in the described glass bottles, at offset distances ranging from 2 mm to 20 mm, in 2 mm increments. For each case, the Raman spectra of the corresponding empty glass bottles are also shown (blue dashed curves, measured in the backscattering mode). Note that the intensity of glass background associated with bottle #1 is much stronger compared with the glass background intensities associated with the other bottles (refer to the intensity scale on the left *y*-axis), although the wall thickness of bottle #1 is not much thicker compared with those of others (listed in Table 1). This implies that there is a considerable variation in glass quality among the transparent glass bottles. In the case of brown-colored bottle #4, the intensity of the glass background is substantially weaker owing to the attenuation of generated glass Raman photons by the brown color (refer to the corresponding visible spectrum in Fig. 1(b)).

For all four bottles, the presence of the glass background is apparent at the shortest offset distance (2 mm), and the intensity decreases with increasing the offset distance. In the case of bottle #1, the glass background is still observable up to the offset distance of 8 mm, owing to the intense glass signal; for the other bottles, the glass background substantially decreased at the offset distances of 4–6 mm. In contrast, in all cases the intensity of the non-overlapping ethanol peak at 878 cm^{-1} is relatively constant (less offset distance-sensitive), although it is expected to decrease owing to the detection of photons further away from the excitation point.

For a more detailed examination, the baselines of the spectra in Fig. 2 were linearly offset to zero at 750 cm^{-1} and then the intensity of the ethanol peak at 878 cm^{-1} was plotted *vs.* the offset distance; the results are shown in Fig. 3. The error bars were obtained based on fifteen measurements performed at each offset distance, as described in the Experimental section. The expected trend of decreasing intensity was only observed in the case of bottle #3; no systematic variations occurred for the other bottles. Since the diameters of bottles #1, #2, and #4 were only slightly larger than that of the detection probe, the number of ethanol photons arriving at the detector was not expected to vary significantly with the offset distance. Moreover, the bottoms of the used bottles were coarsely concave, and their thicknesses were inconsistent, as pointed out in Table 1; therefore, the propagation of individual photons could vary during the passage through the bottoms of different bottles, increasing the uncertainty in photon propagation. This can explain the non-systematic intensity variations that were observed for bottles #1, #2, and #4. Because the diameter of bottle #3 was considerably larger (and the distri-

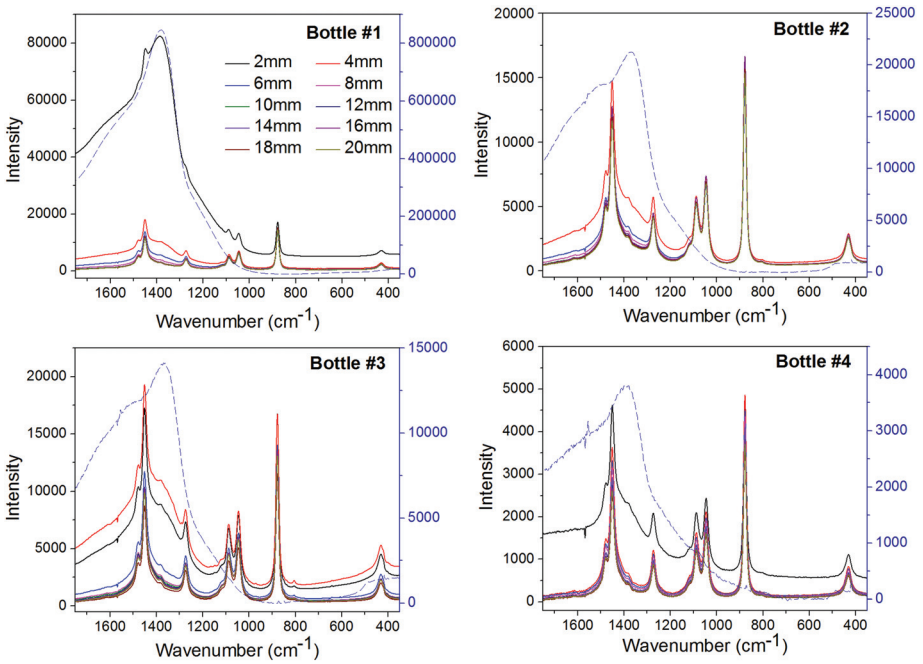

Fig. 2 APO Raman spectra of the 66% ethanol solution housed in the four different glass bottles, collected by varying the offset distance from 2 to 20 mm, in 2 mm increments. In each plot, the Raman spectra of the corresponding empty glass bottle (blue dashed curves), measured in the back-scattering mode, are also shown (the scales are shown on the right-side *y*-axes).

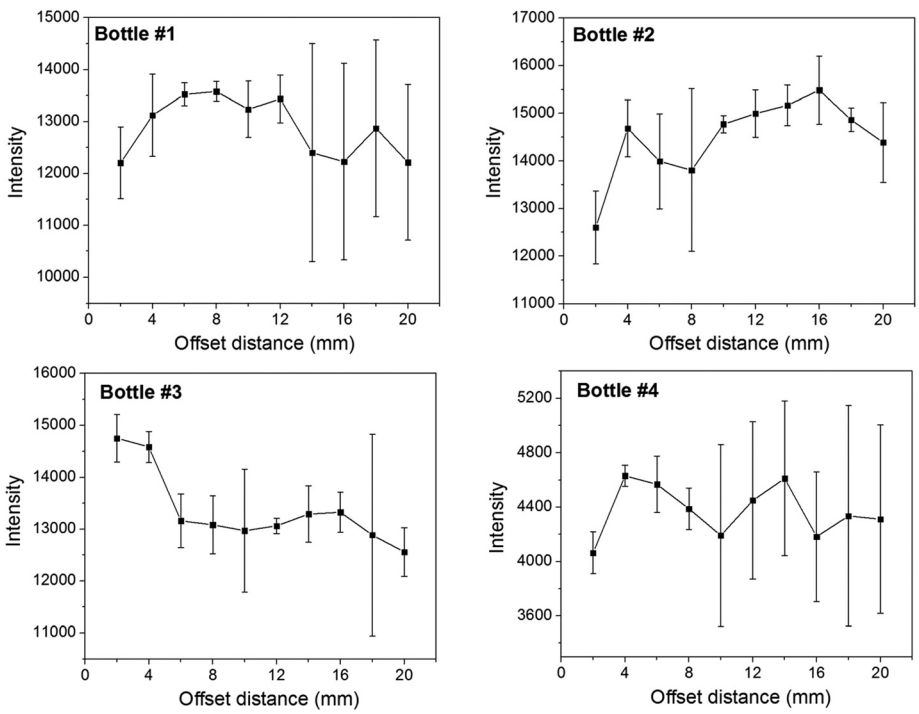

Fig. 3 Peak intensities (at 878 cm^{-1}) of the 66% ethanol solution housed in the four different glass bottles, at the offset distance varying from 2 mm to 20 mm, in APO measurements.

bution of ethanol photons was accordingly broader than the diameter of the detection window), the variability in the number of arriving ethanol photons increased with increasing the offset distance. Therefore, the tendency of intensity to decrease with increasing offset distance became more noticeable.

To estimate the variation of the glass background intensity relative to the intensity of the ethanol peak at each offset distance, we calculated the ratio of the magnitude of the ethanol peak at 878 cm^{-1} to the magnitude of the glass peak at 1380 cm^{-1} (hereafter denoted as $I_{ethanol}/I_{glass}$); the results are shown in Fig. 4. Smaller values of $I_{ethanol}/I_{glass}$ correspond to the stronger contribution of the glass background relative to the ethanol signal. In all four cases, $I_{ethanol}/I_{glass}$ steeply increased at short offset distances and started to level off around the offset distances of 12–16 mm. In the measurements employing the three different transparent glass bottles, the glass background nearly disappeared at sufficiently long offset distances (*e.g.*, 16 mm); on the other hand, for the brown-colored glass bottle, the glass background signal was barely significant when the offset distance was 12 mm.

The normalized Raman spectra of 66% ethanol housed in different bottles acquired at different offset distances of 2 mm, 8 mm, and 16 mm are shown in Fig. 5. For the normalization, the baseline-corrected spectra at five different wavenumbers (1750, 960, 750, 700, and 350 cm^{-1}) were divided by the corresponding peak area in the 1750–350 cm^{-1} range. With the offset distance of 2 mm, the glass background was relatively dominant for bottles #1 and #2. The weaker glass background in the case of bottle #3 at the same offset distance could be attributed to the fact that the detector position was further away from the illumination point, where the generated glass photons were mostly localized, owing to the larger bottle size. The spectral features were nearly the same at the offset distance of 16 mm; yet, in the case of the brown-colored bottle minutely different peak intensities were obtained, because the absorption of ethanol Raman photons by the brown-colored glass was wavelength-dependent for wavelengths longer than 785 nm (excitation wavelength), as shown in Fig. 1(b).

To quantitatively evaluate the ability of the proposed APO scheme to yield pure spectral features of housed samples, we used a hit quality index (HQI), which is a numerical index that captures the correlation (degree of spectral matching) between two spectra. The HQI is unity when two spectra match perfectly. A more detailed description of the HQI can be found in relevant publications.[20–22] In the present study, the Raman spectrum of the same ethanol sample housed in a quartz cuvette was initially chosen as a reference spectrum, because quartz does not generate any Raman background. Next, the HQI values of the APO spectra collected at the offset distance of 16 mm were calculated against the reference spectrum. The resulting HQI values were 0.984, 0.989, 0.989, and 0.981 for bottles #1, #2, #3, and #4, respectively. All of the HQI values were very high and close to one. Taken together, these results demonstrate that at a sufficiently long offset distance the acquired spectra of the contained ethanol sample have highly similar spectral features, owing to the suppression of the glass background, even though four different glass bottles were used for housing the sample.

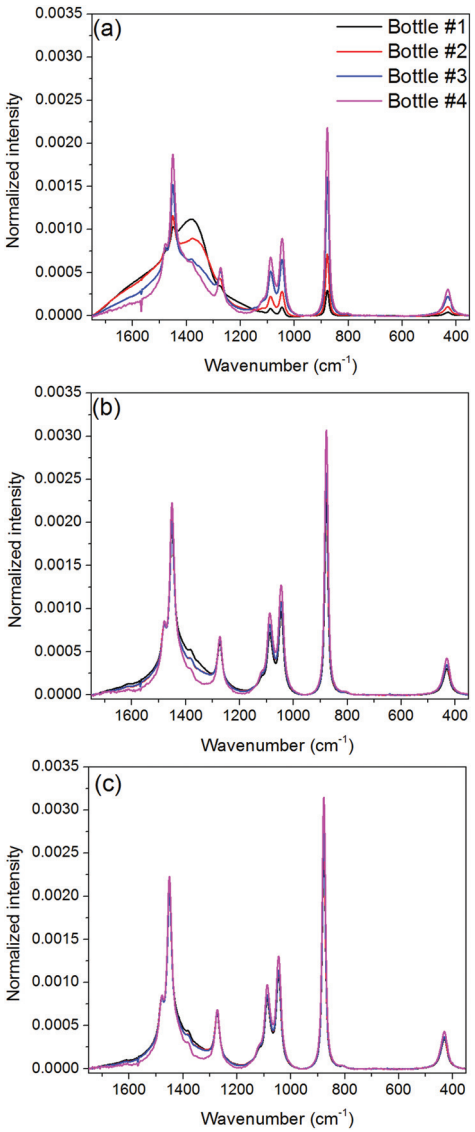

Fig. 5 Normalized Raman spectra of the 66% ethanol housed in the four different bottles, measured at the offset distances of 2 mm (a), 8 mm (b), and 16 mm (c).

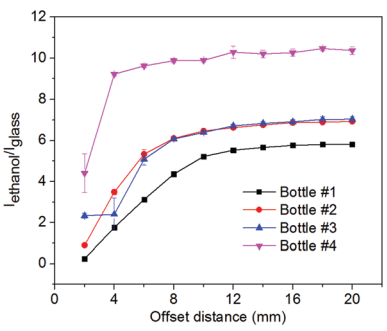

Fig. 4 Ratios of the ethanol peak intensity at 878 cm^{-1} to the glass peak intensity at 1380 cm^{-1} ($I_{ethanol}/I_{glass}$) for APO measurements of the 66% ethanol solution housed in the four different glass bottles, with varying the offset distance from 2 to 20 mm.

Monte Carlo simulation to investigate the propagation of Raman photons in ethanol-containing glass bottles

The Monte Carlo simulation was performed to explain the observed experimental results as well as to visualize photon distributions in the ethanol contained bottles. Fig. 6 shows the three-dimensional distributions of generated Raman photons in the employed bottles. The plots in the left and right columns show the distributions of glass and ethanol photons, respectively, when the offset distance is 12 mm. The cylindrical green lines indicate each glass bottle with the relevant physical dimensions. The cone in each case describes the photon-detection volume generated by the curved glass bottom as described earlier. The experimentally determined focal length of each bottle was employed to construct the detection cone. It is worth noting that the height of the cone in bottle #4 is much smaller due to the shorter focal length. The tiny dots correspond to either glass or ethanol Raman photons, which are present inside the cone. For easier comparison, the plots showing all generated photons (outside and inside the cone) on the same domain are shown in Fig. S2 (ESI†). As is shown, the glass photons are much more localized on the left side, as expected; on the other hand, the ethanol photons are widely distributed throughout the bottles. Therefore, the cone-shaped detection volume is advantageous to physically exclude the generated glass photons due to the sloped top, and a longer offset is additionally effective to decrease the number of glass photons present inside the detection cone.

Fig. 7 shows the number of counted Raman photons in the detection cone obtained by the Monte Carlo simulation at the offset distances from 2 to 20 mm (2 mm increments). The distal distance at each offset distance indicates the horizontal distance between the laser-illuminated point (outer surface of the side wall of the bottle, equally zero distal distance) and the location of interest. The plots in the left and right columns display the counted glass and ethanol photons, respectively. In the case of bottle #1, the numbers of counted glass photons are greater than those in the other cases (refer to the scale of the *z*-axis) since the bottom of the detection cone (diameter: 25.4 mm) is closest to the bottle wall due to the smallest bottle diameter (27.4 mm). The glass photons are much more localized around the distal distances up to 2.5 mm and the number of detected glass photons decreases as the offset distance becomes longer, since the cone-shape detection volume becomes further away from the center of generated glass photons in this situation. In contrast, the decrease in the number of detected ethanol photons with the increase of offset distance is rather insignificant. Since the ethanol photons are widely distributed over the bottle, the number of detected ethanol photons is much less sensitive to the offset distance.

In comparison with the above result, similar trends are observed in the case of bottle #2 except for the smaller numbers of detected glass photons at each offset distance. Since the diameter of bottle #2 is 2.5 mm large than that of bottle #1, the bottom of the detection cone becomes 1.25 mm further away from the center of glass photons. Therefore, a smaller number of glass photons are subsequently detected under this configuration. Meanwhile, a similar tendency is observed in the detection of ethanol photons. In the case of bottle #3 (the largest bottle), the numbers of both detected

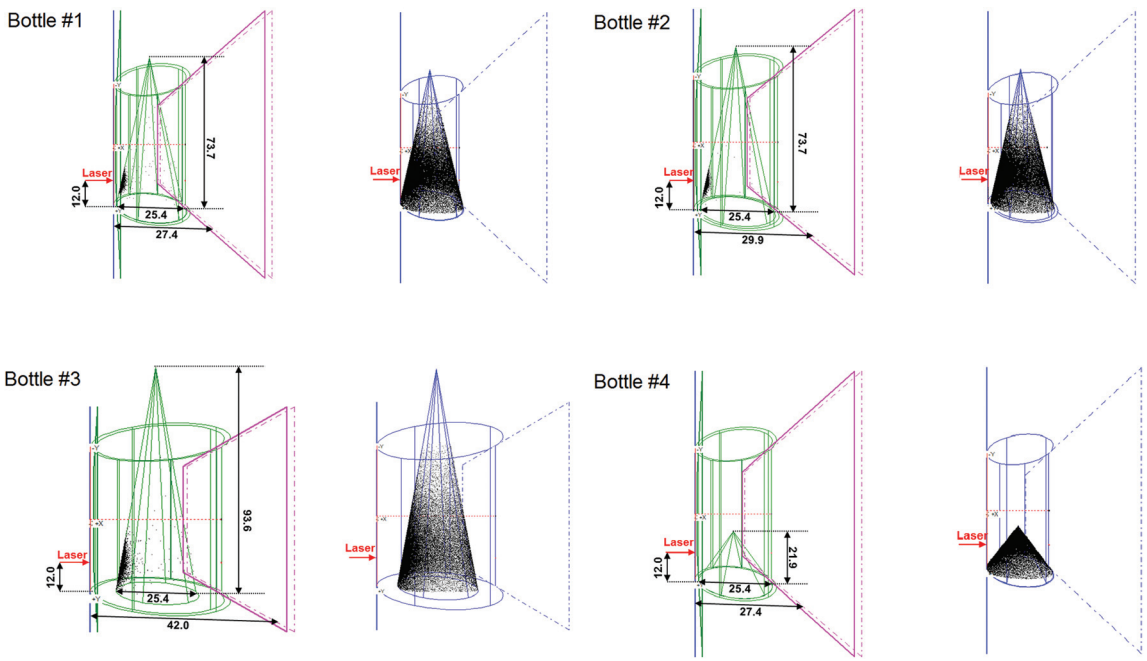

Fig. 6 Three-dimensional distributions of Raman photons inside the detection cone in the measurements of 66% ethanol solution housed in the four different glass bottles (offset distance: 12 mm). The plots in the left and right columns show the distribution of the glass and ethanol photons, respectively. All dimensions are in units of mm.

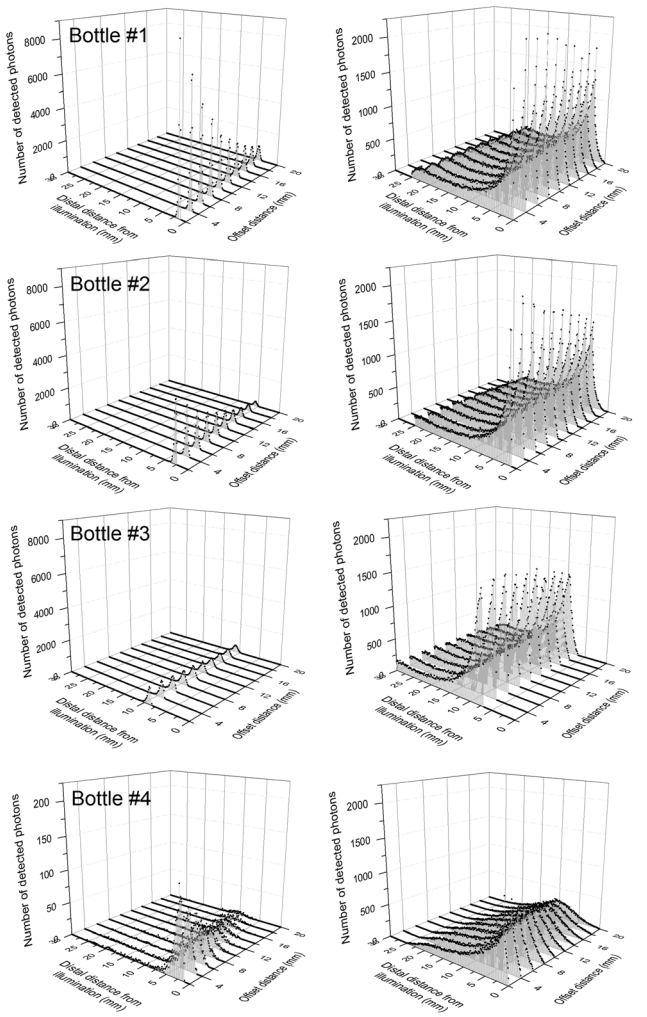

Fig. 7 The number of counted Raman photons in the detection cone obtained by the Monte Carlo simulation at the offset distances from 2 to 20 mm (2 mm increments). The distal distance at each offset distance indicates the horizontal distance between the laser-illuminated point (outer surface of the side wall of the bottle) and the location of interest. The plots in the left and right columns display the counted glass and ethanol photons, respectively.

glass and ethanol photons are further decreased as expected. In particular, the number of detected glass photons is substantially smaller in comparison with those in the cases of bottle #1 and #2, while it also decreases with the increase of offset distance. It is notable that the numbers of ethanol photons at the tested offset distances are quite similar (offset distance-insensitive). The longest focal length provided by the bottom generates the highest detection cone (height: 93.6 mm, refer to Fig. 6), so the number of detected ethanol photons is relatively less sensitive to the change of offset distance.

It is also expected that a detection cone with a smaller height is more advantageous to physically escape from the mass of glass photons, such as brown-colored bottle #4 providing the shortest focal length as shown in Fig. 6. Therefore, $I_{ethanol}/I_{glass}$ in the case of bottle #4 was considerably higher even at the offset distances of 2 and 4 mm in comparison with the other cases. Also, based on the simulation, the numbers of both glass and ethanol photons are much smaller due to the higher absorption of photons by brown color, while the trend of decreasing intensity with lengthening of the offset distance is the same as the other cases.

Overall, the simulation results were supportive in explaining the observations in Fig. 4. The shape of the detection cone and the offset distance were key factors governing the efficiency of rejecting the glass photons against ethanol photons in spectral acquisition. For all 4 cases, the sufficient offset distances such as 14 and 16 mm drove to acquire Raman spectra of the contained ethanol sample with minimized glass background. The curved bottom of the glass vial enabling forming the conical detection volume was the main source for minimizing the glass background in the sample spectra. As the offset distance becomes longer, the detection cone is more effectively away from the mass of glass photons and the rejection of glass photons becomes realized. If the conical detection cone is not formed, the performance of the APO scheme would somewhat degrade.

Conclusion

The usability of the APO scheme for producing distinct spectral features of a sample with minimized glass background, in direct Raman measurements performed on a sample containing glass bottle, was demonstrated here. It is reasonable to expect that an optimal offset distance minimizing the glass background would vary depending on different factors, such as the sample turbidity, the container color and size, the photon detection area, and the location of a detector. Turbidity will make the photon distribution broader, so the sample photons would overlap more with the photons generated from a container. The degree of photon attenuation will vary depend on the container color as well as the laser wavelength. Also, when an employed container is large, the exclusion of generated container photons would be easier as shown in this study. If a detector is located further away from the container wall, the rejection of container photons would be more facile, while the decrease of sample peak intensity should be simultaneously considered. Overall, the effectiveness of the APO scheme is inter-crossly governed by the mentioned as well as other factors.

Although only four bottles of different sizes, including one colored bottle, were employed in this study, the mechanism for avoiding glass photons in the APO scheme was clearly explained and supported by Monte Carlo simulation. The present findings are likely to significantly contribute to the understanding of APO measurements, especially when this method is applied for the analysis of samples housed in various containers with different optical arrangements. Future research will aim at expanding the evaluation of the APO scheme by varying the above-mentioned parameters. In addition, direct quantification of housed sample concentration

would be feasible since the reproducibility is good as indicated by the magnitude of error bars shown in Fig. 4.

Conflicts of interest

There are no conflicts to declare.

Acknowledgements

This research was supported by the Basic Science Research Program through the National Research Foundation of Korea (NRF) funded by the Ministry of Science, ICT & Future Planning (NRF-2018R1A2B2002662).

Notes and references

1 P. Matousek, I. P. Clark, E. R. C. Draper, M. D. Morris, A. E. Goodship, N. Everall, M. Towrie, W. F. Finney and A. W. Parker, *Appl. Spectrosc.*, 2005, **59**, 393–400.
2 P. Matousek, M. D. Morris, N. Everall, I. P. Clark, M. Towrie, E. Draper, A. Goodshi and A. W. Parker, *Appl. Spectrosc.*, 2005, **59**, 1485–1492.
3 M. V. Schulmerich, W. F. Finney, R. A. Fredricks and M. D. Morris, *Appl. Spectrosc.*, 2006, **60**, 109–114.
4 V. S. Matthew, F. F. William, P. Victoria, D. M. Michael, M. V. Thomas and A. G. Steven, *Proc. SPIE*, 2006, **6093**, 60930O.
5 C. Eliasson and P. Matousek, *Anal. Chem.*, 2007, **79**, 1696–1701.
6 P. Matousek, *Appl. Spectrosc.*, 2006, **60**, 1341–1347.
7 M. V. Schulmerich, K. A. Dooley, M. D. Morris, T. M. Vanasse and S. A. Goldstein, *J. Biomed. Opt.*, 2006, **11**, 060502.
8 M. V. Schulmerich, K. A. Dooley, T. M. Vanasse, S. A. Goldstein and M. D. Morris, *Appl. Spectrosc.*, 2007, **61**, 671–678.
9 P. Matousek, *Chem. Soc. Rev.*, 2007, **36**, 1292–1304.
10 C. Eliasson, N. A. Macleod and P. Matousek, *Anal. Chim. Acta*, 2008, **607**(1), 50–53.
11 M. Bloomfield, D. Andrews, P. Loeffen, C. Tombling, T. York and P. Matousek, *J. Pharm. Biomed. Anal.*, 2013, **76**, 65–69.
12 B. Zachhuber, C. Gasser, E. H. Chrysostom and B. Lendl, *Anal. Chem.*, 2011, **83**, 9438–9442.
13 P. Matousek, *Central Laser Facility Annual Report*, 2006/2007.
14 T. M. Guy, S. Bonthron and D. Crawford, *Proc. SPIE*, 2013, **8901**, 890104.
15 P. K. Duy, K. Chang, L. Sriphong and H. Chung, *Anal. Chem.*, 2015, **87**, 3263–3271.
16 F. F. M. De Mul, M. H. Koelink, M. L. Kok, P. J. Harmsma, J. Greve, R. Graaff and J. G. Aarnoudse, *Appl. Opt.*, 1995, **34**, 6595–6611.
17 IUPAC, Compendium of Chemical Terminology, 2nd ed. (the "Gold Book"). Compiled by A. D. McNaught and A. Wilkinson. Blackwell Scientific Publications, Oxford (1997). XML on-line corrected version: http://goldbook.iupac.org(200(6-) created by M. Nic, J. Jirat, B. Kosata; updates compiled by A. Jenkins. ISBN 0-9678550-9-8. DOI: 10.1351/goldbook.
18 F. F. M. De Mul, Monte-Carlo Simulation of Light Transport in Turbid Media, in *Handbook of Coherent Domain Optical Methods, Biomedical Diagnostics, Environment and Material Science*, ed. V. V. Tuchin, Kluwer Publishers, Dordrecht, The Netherlands, 2004, p. 465.
19 F. F. M. De Mul, M. H. Koelink, L. M. Kok, P. J. Harmsma, J. Greve, R. Graaff and J. G. Aarnoudse, *Appl. Opt.*, 1995, **34**, 6595–6611.
20 *Spectral ID Users Guide*, Galactic Industries Corporation, Salem, NH, 1998, p. 1198.
21 M. G. Connie, D. R. Jason, A. Sergey, F. B. Lucinda and F. K. John, *J. Pharm. Biomed. Anal.*, 2012, **61**, 191–198.
22 D. R. Jason, J. W. Benjamin, F. B. Lucinda and F. K. John, *Anal. Chem.*, 2011, **83**, 4061–4067.